Orbit related sea level errors for TOPEX altimetry at seasonal to decadal time scales

Saskia Esselborn[1], Sergei Rudenko[1,2], Tilo Schöne[1]

[1]GFZ German Research Centre for Geosciences, Potsdam, 14473, Germany
5 [2]Deutsches Geodätisches Forschungsinstitut (DGFI-TUM), Technische Universität München, Munich, 80333, Germany (since August 2016)

Correspondence to: Saskia Esselborn (Saskia.Esselborn@gfz-potsdam.de)

Abstract. Interannual to decadal sea level trends are indicators of climate variability and change. A major source of global
10 and regional sea level data is satellite radar altimetry, which relies on precise knowledge of the satellite's orbit. Here, we assess the error budget of the radial orbit component for the TOPEX/Poseidon mission for the period 1993 to 2004 from a set of different orbit solutions. Upper bound errors for seasonal, interannual (5 years), and decadal periods are estimated on global and regional scales based on radial orbit differences from three state-of-the-art orbit solutions provided by different research teams (GFZ, GSFC, and GRGS). The global mean sea level error related to the orbit is of the order of 7 mm (more
15 than 10 % of the sea level variability) with negligible contributions on the annual and decadal time scale. In contrast, the orbit related error of the interannual trend is 0.1 mm/year (18 % of the corresponding sea level variability) and might hamper the estimation of an acceleration of the global mean sea level rise. For regional scales, the gridded orbit related error is up to 11 mm and for about half the ocean the orbit error accounts for at least 10 % of the observed sea level variability. The seasonal orbit error amounts to 10 % of the observed seasonal sea level signal in the Southern Ocean. At interannual and
20 decadal time scales, the orbit related trend uncertainties reach regionally more than 1 mm/year. The interannual trend errors account for 10 % of the observed sea level signal in the Tropical Atlantic and the south-eastern Pacific. For decadal scales, the orbit related trend errors are prominent in a couple of regions including: South Atlantic, western North Atlantic, central Pacific, South Australian Basin, and Mediterranean Sea. Based on a set of test orbits calculated at GFZ, the sources of the observed orbit related errors are further investigated. Main contributors on all time scales are uncertainties in Earth's time
25 variable gravity field models and on annual to interannual time scales discrepancies of the tracking station sub-networks, i.e., SLR and DORIS.

1 Introduction

Sea level is an important indicator of climate variability and change. Based on tide gauge data using different techniques, the global mean sea level rise for the last century is estimated to be 1.2-1.9 mm/year (Douglas, 1997; Church and White, 2011; Jevrejeva et al., 2008, 2014; Hay et al., 2015). Based on satellite altimetry data since 1993, the current rate of global mean sea level has been estimated to be more than 3 mm/year (Cazenave et al., 2014; Ablain et al., 2015). The main sources of the current rise are thermal expansion of the sea water and melting of glaciers and ice sheets. At interannual time scales, changes of terrestrial water storage imprint additionally on the global mean sea level (Llovell et al., 2011). Recent work has focussed on the detectability of accelerations in global mean sea level trends during the last decades (Watson et al., 2015; Fasullo et al., 2016). Regionally, sea level rates during the last 24 years show higher variability, they range from -1 mm/year to more than 10 mm/year. They are mainly linked to regional changes in the oceans density field, which might be induced by internal ocean variability, atmosphere-ocean interaction, or influx of freshwater. Satellite altimeters are a unique source of global and regional sea level data and are available continuously since the beginning of the 1990s. Precise orbits of altimetry satellites are a precondition for global and regional mean sea level investigations (Rudenko et al., 2012; Rudenko et al., 2014) and errors related to precise orbit determination (POD) are demonstrably one of the major error sources for global and regional sea level products (Ablain et al., 2015). A detailed description of the main factors contributing to the radial orbit errors is given by Fu and Haines (2013). The orbit errors have typically long-wavelengths and may contain systematic contributions at seasonal to decadal timescales.

Couhert et al. (2015) investigated the main contributions to the radial orbit error budget for the Jason-1 and Jason-2 series based on Geophysical Data Records (GDR)-D at seasonal to decadal time scales for the second altimetry decade (2002-2013). According to their analysis, the orbit related uncertainty of the global mean interannual and decadal trends is less than 0.1 mm/year. As main factors for regional errors they identified: contributions from tracking data and from reference frame (up to 8 mm) at seasonal time scales, contributions from tracking data (up to 3 mm/year) and Earth's time variable gravity field (up to 2 mm/year) at interannual time scales, and contributions from tracking data (up to 2 mm/year) and Earth's time variable gravity field (up to 1.5 mm/year) at decadal time scales. A correspondent assessment for the first altimetry decade (1992-2001) has been still missing and is the rationale of this paper.

We assess the error budget of the radial orbit component for the TOPEX/Poseidon mission for the period 1993 to 2004 from a set of different orbit models. We have chosen TOPEX/Poseidon, since it is the reference altimetry mission used in the European Space Agency's (ESA) Climate Change Initiative (CCI) Sea Level project over this time span (Ablain et al., 2016). We assess the upper bound estimates of the radial orbit error budget at regional and global scales at seasonal, interannual, and decadal time scales by the analysis of three state-of-the-art orbit solutions provided by different research teams from the German Research Centre for Geosciences (GFZ), the Groupe de Recherche de Geodesie Spatiale (GRGS), and the Goddard Space Flight Centre (GSFC). In our further analyses, we use test orbits calculated at GFZ to investigate the impact of

uncertainties of the tracking station sub-networks, of the reference frame, and of the Earth's time variable gravity field models on the radial orbit component, and hence the derived sea level.

A detailed description and assessment of the analysed orbits as well as specifications of the altimeter data processing are given in Sect. 2. Sect. 3 describes the methods implemented to assess the upper bound orbit errors for the different time scales and the corresponding results for global and regional scales. The main findings are summarized and discussed in Sect. 4.

2 Data

2.1 Description of the analysed orbit solutions

Our aim is to assess the range and the characteristics of radial orbit errors on regional and global scales. Therefore, three independent state-of-the-art orbit solutions available for the TOPEX/Poseidon mission are analysed. All orbit solutions are derived in the International Terrestrial Reference Frame (ITRF) 2008 reference frame (Altamimi et al., 2011) and use Satellite Laser Ranging (SLR) and Doppler Orbitography and Radiopositioning Integrated by Satellite (DORIS) tracking data, but are based on different software and on distinct models including different time variable gravity field models. The actual multi-mission GFZ orbit solution VER11 (Rudenko et al., 2017) is used as a reference in this paper and is called REF hereafter. The GSFC std1504 orbit (Lemoine et al., 2010; Beckley et al., 2015) has been chosen by the ESA CCI Sea Level Phase 2 project and differs in many aspects from the GFZ orbit, regarding software as well as the suite of implemented models including another Earth's gravity field model. As the third model, we have chosen the GRGS orbit solution (Soudarin et al., 2016), which is derived using models similar to those of the GFZ solution. The main models used for GFZ REF, GRGS, and GSFC std1504 orbits are described in Table 1. The main differences in these three orbit solutions are related to the choice of the Earth's time variable gravity field models, ocean tide model, modelling of non-tidal atmospheric and oceanic gravity, and the treatment of geocenter variations in station displacements.

To estimate the orbit related radial orbit error budget due to the most significant factors, we have derived four test orbits based on the GFZ REF orbit. The tested factors include the consistency of the tracking data networks, the Earth's time variable gravity field model, and the realization of the terrestrial reference frame. For each case, the same background models and estimated parameters were used as for the REF orbit, except for those that represent the changes for the specific test case. The four test orbits are:

- SLR orbit: derived by using SLR tracking observations only,
- DORIS orbit: computed by using DORIS tracking observations only,
- ITRF14 orbit: calculated by using the information on station positions and velocities from ITRF2014 (Altamimi et al., 2016) instead of ITRF2008,

- Geoid orbit: obtained by using EIGEN-6S2 (Rudenko et al., 2014) Earth's gravity field model instead of EIGEN-6S4 model (Förste et al., 2016). Note that the Geoid orbit is based on the same gravity field model as the GRGS orbit.

2.2 TOPEX altimeter data

In order to assess the orbit accuracy at crossover points and to relate the estimated errors to the total variability of the sea level data, along-track TOPEX Sea Level v1.1 ECV data (Ablain et al., 2016) released from the ESA CCI Sea Level project has been included in the analyses. The along-track data has been corrected for all instrumental and geophysical effects by the state-of-the-art models provided with the data. However, for some corrections update models were applied. These include: the GSFC std1504 orbits, EOT11a ocean tides and loading tides (Savcenko and Bosch, 2012), solid earth tides following the IERS conventions, and updated GPD+ wet tropospheric corrections (Fernandes and Lazaro, 2016). The processing of the data, the crossover point and collinear analyses as well as the interpolation to a regular grid were performed using GFZ's Altimeter Database and Processing System (ADS) Central (Schöne et al., 2010).

2.3 Evaluation of the orbit solutions

In the following, the performance of the analysed orbits is evaluated. For the GFZ orbit solutions, the consistency with tracking data and at arc overlaps is assessed. Table 2 provides the main results of precise orbit determination of the GFZ reference and test orbits, namely, the average values of SLR and DORIS RMS fits, radial, cross-track, and along-track two-day arc overlaps, illustrating the internal orbit consistency in these directions, and the number of the arcs used to compute these values for the reference and four test orbits. Smaller values of arc overlaps and observation fits, when using the same observation types and weighting between them, indicate improved orbit quality. Reduced radial arc overlaps characterise reduced radial orbit error. SLR observations were used at all 494 orbital arcs of four GFZ orbits, except for the DORIS orbit for which no SLR observations were used at all. Since DORIS data are available for TOPEX/Poseidon only until October 31, 2004, these data were used at 433 orbital arcs preceding this date, except for the SLR orbit for which no DORIS observations were used at all. All orbital arcs for GFZ orbits are manoeuvre-free. Thus, two-day arc overlaps were computed for 433 overlaps for the REF, ITRF14, and Geoid orbits. In case of the SLR and DORIS orbits, a few gaps in the observations caused radial arc overlap larger than 0.5 m. Those arc overlaps have been excluded from the statistics resulting in less arc overlaps shown for these orbits in Table 2.

Figures 1 and 2 provide information on the quality of the reference and tests orbits. The three orbits derived using SLR and DORIS observations provide comparable levels of average SLR RMS fits (1.96 – 1.97 cm, Fig. 1). The smallest average SLR RMS fits (1.59 cm) are obtained with the orbit based on SLR observations only. This is related to the weighting of observations used: 3 cm for SLR observations and 0.05 cm/s for DORIS observations. Among four orbits derived using DORIS observations, a slightly increased average value of DORIS RMS fits (0.04795 cm/s) is obtained for the DORIS orbit

derived using only DORIS observations, while the three orbits derived using SLR and DORIS observations (REF, ITRF14, and Geoid) show comparable average values of DORIS RMS fits (0.04775 – 0.04778 cm/s). Fig. 2 shows two-day arc
125   overlaps in the radial direction depending on the type of observations used for precise orbit determination: SLR-only, DORIS-only and SLR+DORIS data. The smallest average value of the radial overlaps (0.88 cm) is obtained using DORIS-only observations. The radial arc overlaps of the TOPEX/Poseidon orbit derived using only SLR data are 1.95 times larger than those of the orbit derived using only DORIS data (Fig. 2). Using the reference frame ITRF2014 instead of ITRF2008 eliminates many outliers in the radial arc overlaps (Fig. 2) and therefore reduces the average value of the radial overlaps
130   from 0.90 to 0.84 cm.

For all orbit solutions, a crossover point analysis for the period April 1993 to November 2004 has been performed based on the altimeter data described above. Differences between values of ascending and descending tracks at crossover points are caused by oceanic variability and errors related to the measurements, the orbit, and the applied corrections. Since in our study errors related to the measurements and the applied corrections and oceanic variability are always identical, here,
135   smaller absolute mean differences and decreased RMS values at crossover points are indicative for increased orbit quality. The median of the time series of global mean height differences and RMS values at the crossover points are provided in Table 3. The smallest ascending/descending differences (-1.6 mm) and as well the lowest RMS values (49.5 mm) at the crossover points are reached by the GSFC orbit solution. The mean global ascending/descending differences are -3.1 mm for the GFZ REF and 2.9 mm for the GRGS orbit solutions. However, while the RMS value of the GFZ REF solution (49.8 mm)
140   is comparable to the one of the GSFC, the GRGS orbit solution shows degraded performance (51.3 mm RMS). The median of the global mean ascending/descending differences is -2.6 mm for the SLR and -4.7 mm for the DORIS orbits. Both orbit solutions show degraded performance (51.1/50.7 mm RMS) with respect to the REF solution. This shows that using SLR and DORIS observations together improves the orbit quality considerably, even though the DORIS observations seem to aggravate the mean differences between ascending and descending tracks. Using ITRF2014 instead of ITRF2008 does not
145   change the crossover point statistics. The Geoid orbit solution exhibits clearly improved ascending/descending differences (-2.1 mm) and as well a slight reduction of the RMS values.

3 Estimation of the orbit related sea level error

Sea level is varying on typical temporal and spatial scales, that are often connected to the driving processes. At the same time, orbit errors are not randomly distributed but exhibit also typical temporal and spatial pattern. Here, we apply statistical
150   methods in order to assess upper bound errors related to the orbit solutions for global and regional sea level at seasonal to decadal time scales.

3.1 Methods

In order to estimate upper limits for orbit related errors in sea level height, the differences between the radial components of the GFZ REF orbit and the two independent orbit solutions (GSFC and GRGS) have been analysed. To assess the effect of

155   uncertainties in the reference system, in the realisation of the tracking station networks, and in Earth's time variable gravity on the radial error budget, we have evaluated the differences of the radial orbit components between the GFZ's REF and ITRF14, SLR, DORIS, and Geoid test orbits. Since the radial orbit components map directly to the derived sea level heights, we consider the differences presented here to represent estimates of the orbit related sea level error.

The differences of the radial orbit components at the time of the altimetry measurement (1 Hz, ~6.7 km on ground) are

160   calculated and interpolated to a global 1°x1° grid for every cycle (9.92 days). In general, we merge both, ascending and descending, tracks in our calculations. In addition, we analyse ascending and descending tracks for some orbit combinations separately.

For the regional analyses, starting from the gridded radial orbit differences, the RMS values relative to the local temporal mean are calculated for each grid point over the entire time series. Decadal trends, annual and semi-annual signals, and the

165   corresponding formal errors are estimated by a least-square fit. As a measure for errors at interannual time scales, we calculate the RMS of the five-years running trend series of the radial orbit differences at each grid point. Regional upper bound errors are guessed from the corresponding maximum RMS values over the ocean at the 1°x1° grid.

For the global analyses, the gridded radial orbit differences are averaged (with area weighting) over the ocean (±67° latitude). Starting from these global mean height differences, global mean RMS, decadal trend, annual cycle, and the RMS of

170   the five-years running trends series are derived, based on the same methods as used for the regional analyses. Global mean RMS values per cycle are calculated as the square root of the spatial mean of the radial orbit differences at each grid point over the ocean for the respective cycle.

In order to relate the estimated errors to the total variability of the sea level data, TOPEX altimeter data has been included as well. The data and the processing is described in Sect. 2.2. From the gridded sea level anomalies, seasonal, interannual and

175   decadal trends were derived using the methods described above.

3.2. Global mean errors

In the following, we investigate the orbit related global sea level error, differentiating between the total error and its annual, interannual, and decadal components. The time series of the global mean RMS of gridded radial orbit differences per cycle are shown in Fig. 3 for all orbit solutions relative to GFZ's REF orbit. The largest differences occur between the REF and the

180   GRGS orbits, the smallest changes occur for the ITRF14 test orbit. Most orbit differences are dominated by sub-seasonal variability, only the Geoid and ITRF14 orbit differences are governed by seasonal and decadal periods. For the Geoid, GSFC, and GRGS orbits, the RMS series exhibit a seasonal cycle, which is an indication for seasonal orbit differences on regional scales. The orbit errors derived from the analysis of the global mean orbit difference series over the oceans are

summarized in Table 4 for all orbit models together with the corresponding absolute sea level values. The global mean radial orbit differences between the REF and GRGS (GSFC) orbits amount to 7.0 (5.4) mm, which corresponds to more than 10 % of the global mean sea level variability of 52.5 mm. The restriction to one tracking station sub-network leads to large changes of the orbit, for the DORIS (SLR) orbit solution the RMS values of the radial differences with respect to the REF orbit amount to 5.1 mm (4.2 mm), which is almost of the size of the estimated upper bound orbit errors. This highlights the importance of manifold, precise, and consistent tracking data for accurate global mean sea level estimates. The substitution of the Earth's gravity field model (EIGEN-6S4 by EIGEN-6S2) and the ITRF realization (ITRF2008 by ITRF2014) accounts for 2.0 mm and 1.1 mm, respectively, of the mean orbit errors. The annual component of the global mean orbit differences is not included in Table 4, since it is not significant. The time series of the five-years running trends of the global mean radial orbit differences over the ocean are shown in Fig. 4 for the various orbit combinations. All curves range between ±0.2 mm/year and show at least one zero-crossing, which is consistent with small changes of the decadal trends. The five-years running trends for the global mean sea level are much larger, they range between 4 mm/year at the beginning of the time series and 2 mm/year at the end (not shown). At the beginning of the time series, the GSFC and GRGS solutions are close to each other and both suggest smaller interannual trends than the GFZ solution before 1998. After that, trends derived from GFZ and GSFC orbits show good agreement, while the GRGS solution results in somewhat higher trends till 2001. Maximum interannual trend variability of 0.1 mm/year occurs between the REF and GRGS orbits which amounts to almost 20 % of the corresponding value derived for the global mean sea level curve (0.55 mm/year). Since the exclusive use of DORIS tracking station leads to interannual trend variability of 0.1 mm/year, inconsistencies of the tracking stations sub-networks are capable to explain large portions of the observed global mean interannual variability. The errors of the interannual trend variability are for all orbit combinations higher than for the decadal trends. The global mean decadal trends (calculated over the full mission time) are mostly significant but can be further neglected, since they are two orders of magnitude smaller than the observed sea level signal over this period (~3 mm/year).

3.3 Regional errors

The maximum regional errors derived from the analysis of the gridded orbit difference series over the oceans are summarized in Table 5. Regionally, the maximum radial orbit differences on the 1°x1° grid between the REF and GRGS (GSFC) orbits amount to 10.7 (7.4) mm. The exclusive use of only one tracking station sub-network leads to distinct changes with RMS values of 9.3 mm (7.2) mm for the DORIS (SLR) sub-network. This suggests that especially inhomogeneity in the SLR station sub-network has the potential to produce considerable regional orbit errors.

Annual difference signals with respect to the REF orbit are most prominent for the GSFC and GRGS solutions, while they are negligible for the SLR and ITRF14 orbits. The corresponding patterns of annual amplitudes for the differences of REF versus GSFC, GRGS, DORIS, and Geoid orbits are shown in Fig. 5. Plausible sources of the relatively strong signal for the GSFC and GRGS orbit cases are the differences in the used Earth's time variable gravity field models, the use of AOD1B products instead of ECMWF data for the reference orbit, and differences in the annual corrections for station coordinates.

The observed patterns for the GSFC and GRGS orbit differences consist of the superposition of two dipoles oriented north/south and east/west. The east/west oriented dipole pattern coincides with the patterns already shown to be related to the use of AOD1B products (Rudenko et al., 2016) and different Earth's time variable gravity fields for TOPEX/Poseidon POD
220 (Esselborn et al., 2016). The north/south oriented dipole pattern corresponds to variations in the z-component of the reference system which is consistent with annual geocentre motions variations described for the Jason-2 mission by Melachroinos et al. (2013). The same pattern is also observed for the annual signal of the *DORIS minus REF* orbit differences.

The patterns of the interannual variability of the regional trends are shown in Fig. 6 for all orbit differences. The trend errors
225 reach up to 1.2 (0.9) mm/year for the GSFC (GRGS) orbit differences (Table 5). The patterns of the trend variability from the GSFC and GRGS differences show coinciding maxima in the regions around South America and Australia. The differences for the Geoid orbit show similar features even though the absolute trend variability is smaller (up to 0.4 mm/year). For the SLR and DORIS orbit differences, the patterns of interannual variability (Fig. 6) are patchy and oriented along individual tracks. For the ITRF14 solution, the trend variability is slightly increased at high latitudes (up to 0.2 mm/year).

230 The strongest regional changes in the decadal trend (Fig. 7 and Table 5) are observed for the differences between the REF and GSFC orbits (up to 1.0 mm/year). For the GSFC orbit, high absolute decadal trend differences tend to coincide with maximum seasonal differences, but not with maximum interannual variability. The differences between REF and GRGS orbit trends reach 0.7 mm/year at maximum and show similar patterns as the differences between REF and Geoid orbit trends (up to 0.4 mm/year). Here, the patterns of maximum annual amplitudes, interannual and decadal trend differences
235 coincide. The ITRF14 orbit differences drift locally by a rate of up to 0.2 mm/year with positive values in the southern hemisphere and negative values in the northern hemisphere, indicating a drift in the z-component between the reference system realisations. The observed values are in good agreement with the combined change of scale and rate of the z-component of the transformation between ITRF2008 and ITRF2014 (Altamimi et al., 2016). The regional decadal trends for the SLR and DORIS orbit differences are patchy and rather related to particular tracks without consistent long-wavelength
240 behaviour. Higher trends of up to 0.4 mm/year emerge for the DORIS orbit.

Our analysis exhibits large scale patterns of the orbit related error. How do these relate to the patterns of sea level variability? Fig. 8 shows the sea level variability, seasonal signal, interannual and decadal trends derived from ESA CCI TOPEX altimeter data for those regions where the orbit error amounts to at least 10 % of the corresponding sea level value. This allows us to define regions where the orbit related error should be considered when analysing the sea level data. For about
245 half the ocean the orbit error accounts for at least 10 % of the observed sea level variability. This is especially the case for calm oceanic regions, whereas for energetic regions like the Circumpolar Current, Tropical Pacific, and the western boundary currents of the northern hemisphere the dynamic ocean signal is much larger than the orbit error. For the seasonal signal, mainly the Southern Ocean is affected. The influence of the orbit error on the interannual trend variability is important in the Tropical and Subtropical Atlantic and the south-eastern Pacific. The estimation of the decadal trend may be

250   hampered by orbit errors in the following regions: central Pacific, South Atlantic, western North Atlantic, south-eastern Indian Ocean, but also in several marginal seas including the Mediterranean, Red Sea, Yellow Sea and Sea of Japan.

3.4 Differences between ascending and descending tracks

In the following, systematic differences of errors derived from ascending and descending tracks are investigated. It has been described before, that orbit errors might reveal diverging drifts for ascending and descending tracks (e.g., Fu and Haines,

255   2013). From our crossover point analysis (Table 3), we have chosen the three orbit solutions revealing the largest RMS values, i.e., GRGS, DORIS, and SLR. For these orbits solutions, we performed the same analyses as before but separately for ascending and descending tracks. However, in contrast to the previous analysis, we study the difference *Geoid minus GRGS* instead of *REF minus GRGS* in order to exclude the effects of different time variable gravity fields from the results.

The interannual trend variability and decadal trends derived from the analysis of the global mean orbit difference series over

260   the oceans are summarized in Table 6 for the merged, ascending, and descending tracks. If the ascending and descending tracks are analysed separately, the interannual trend variability is increased by about 5 times for the corresponding orbit differences. There are notable discrepancies of the global mean decadal trends (up to 0.3 mm/year) between ascending and descending tracks for the *REF minus SLR*, *REF minus DORIS*, and *Geoid minus GRGS* differences. The most striking feature is that the ascending trends are opposite to the descending trends.

265   The regional patterns of the decadal trend differences for ascending and descending tracks are shown in Fig. 9. The SLR and DORIS orbit differences reveal a striking spread between the decadal trends of the ascending and descending tracks. The trends are opposite for ascending and descending tracks for most areas of the global ocean and reach regional values of up to 0.8 mm/year. Trends for the *REF minus SLR* orbit differences are smaller and opposite to the *REF minus DORIS* orbit ones. The corresponding analysis for the *Geoid minus GRGS* orbit differences, which share the same Earth's time variable gravity

270   field model, shows very similar features as for the DORIS differences. To further investigate the relation between ascending and descending tracks, we calculated the principal components of the gridded orbit difference time series. The pattern of the leading component for all analysed ascending and descending difference grids are large scale and correspond to variations of Earth's pole flattening. The corresponding time series of the ascending and descending series are highly anti-correlated for frequencies lower than 1 year (-0.91 for *REF minus SLR*, -0.95 for *REF minus DORIS*, and -0.87 for *Geoid minus GRGS*).

275   This indicates that discrepancies in the reference systems of the tracking stations (distribution of tracking stations, observation sampling, etc.) might give rise to long-wavelength orbit errors being anti-correlated for ascending and descending tracks. On regional scales, the interannual and decadal trend errors derived from ascending/descending tracks separately can reach twice the values derived from the merged data. Even though such effects tend to cancel, whenever both components are merged, they might still introduce considerable errors in regional studies, that are based on along-track data,

280   e.g. at calibration sites.

4 Summary and Conclusions

We have investigated the radial orbit error budget associated with state-of-the-art orbit solutions over the first altimetry decade (1993-2004). It is crucial to know the accuracy of these early altimeter data in order to judge the reliability of estimations of the acceleration of global mean sea level rise and of long-term sea level trends. For this purpose, we have

285 chosen the TOPEX/Poseidon mission, since it is the reference altimetry mission used in ESA's CCI Sea Level project over this time span. In our analyses, we have focused on the impact of uncertainties of the tracking station sub-networks (SLR and DORIS), of the reference frame, and of the Earth's time variable gravity field models on the radial orbit component, and hence the derived sea level. The estimates of the upper bound radial orbit errors at seasonal, interannual (5 years), and decadal time scales are given in Table 4 for the global mean sea level and in Table 5 for the regional sea level.

290 According to our study, the global mean RMS radial orbit errors for the TOPEX period are of the order of 7 mm, which corresponds to more than 10 % of the global mean sea level variability (52 mm). The global mean annual (seasonal) component of the radial error can be neglected. The orbit related errors of the decadal trends are less than 0.05 mm/year and should not induce any significant artificial global mean sea level trends. However, on time scales of five years the trend variability may reach up to 0.1 mm/year, which amounts to almost 20 % of the corresponding sea level variability

295 (0.55 mm/year), and could potentially hamper the detection of interannual sea level signals from the altimeter data. The major contributions to this error are, most probably, discrepancies of the station sub-networks (DORIS or SLR) used. The contributions of Earth's time variable gravity field model and the ITRF realisation (ITRF2008 vs ITRF2014) to the global mean error are of only minor importance.

For regional scales, the maximum RMS of the gridded radial orbit error is more than 10 mm derived from the two state-of-

300 the-art orbit solutions GFZ REF (VER11) and GRGS. However, this error includes a large fraction of sub-seasonal variability which is not subject of this study. The regional upper bound error of the seasonal signal is 6 mm, of the interannual trend variability 1.2 mm/year, and of the decadal trend 1 mm/year, as estimated from the difference between the GFZ REF and the GSFC std1504 orbit solutions. Errors induced by uncertainties of the Earth's time variable gravity field model are studied on the base of GFZ's Geoid orbit solution. The orbit evaluations show that the Geoid orbit performs

305 slightly better than the REF orbit. Uncertainties of the gravity field model give rise to orbit errors at all analysed periods and the corresponding patterns show close agreement with the ones derived from the GFZ and the external orbit differences. We estimate regional upper bound errors of ~3 mm for the seasonal signal and of 0.4 mm/year for the interannual trend variability and the decadal trend. This accounts for about 60 % of the seasonal, about 30 % of the interannual, and about 40 % of the decadal error which are related to uncertainties of the time variable gravity field models. However, these values

310 might be still underrated due to the similarity of the two time variable gravity field models used for GFZ's REF und Geoid orbit solutions. Orbit errors related to discrepancies between the tracking station sub-networks (distribution of tracking stations, observation sampling, etc.) are studied based on GFZ's SLR and DORIS orbit solutions. Using both SLR and DORIS observations for TOPEX POD together reduces (improves) the RMS of the altimetry single-satellite crossover

differences considerably, though the DORIS observations seem to aggravate the mean differences between ascending and

315 descending tracks. Hence, the restriction to only one tracking station sub-network has considerable regional effects on the orbit solutions. The most significant changes are observed for the DORIS orbit solution suggesting that uncertainties of the SLR station sub-network should have the most prominent effects on the orbit accuracy – at least for GFZ's orbit solutions. This fact is, most probably, related to the weighting factors applied to the observations within the GFZ orbit determination process. The seasonal errors related to the exclusive use of the DORIS tracking station sub-network are maximum at high

320 latitudes (up to 2 mm) and are conform to uncertainties in the z-coordinate of the orbit's reference system. For interannual and decadal time scales, the errors related to the exclusive use of the DORIS tracking station sub-network are patchy and rather oriented along single satellite tracks with most pronounced errors at interannual time scales (up to 0.6 mm/year). However, when using ascending or descending tracks separately, the interannual and decadal trend errors can reach twice the values derived from the merged data. The corresponding large scale patterns correspond to variations of Earth's pole

325 flattening and are anti-correlated for ascending and descending tracks on time scales of more than one year. Even though such effects tend to cancel, whenever both components are merged, they might still introduce considerable errors in regional studies, that are based on along-track data, e.g. at calibration sites. Using ITRF2014 instead of ITRF2008 slightly improves the accuracy of the orbit solution as shown by the orbit evaluation. The contribution of the uncertainties in the ITRF realisation (ITRF2014 versus ITRF2008) to the regional upper bound error is only marginal, with maximum seasonal signals

330 of 0.4 mm and interannual to decadal signals of 0.2 mm/year.

Our analysis exhibits large scale patterns of the orbit related error. Errors for interannual to decadal sea level trends of more than 1 mm/year might hamper the interpretation of the observed sea level variability from altimetry, at least apart from the large oceanic currents. In order to define regions where the orbit related error should be considered when analysing sea level data from TOPEX, we have determined areas with orbit errors of at least 10 % of the corresponding sea level value. Taking

335 into account the total orbit related error, about half the ocean is affected. For the seasonal signal, mainly the Southern Ocean is concerned. Critical regions for the estimation of the interannual variability are the Tropical and Subtropical Atlantic and the south-eastern Pacific. For decadal scales, the orbit related trend errors are prominent in a couple of regions including: South Atlantic, western North Atlantic, central Pacific, and south-eastern Indian Ocean, but also several marginal seas including the Mediterranean, Red Sea, Yellow Sea and Sea of Japan.

340 Our estimation of the global mean upper bound orbit errors for the first altimetry decade is in line with the numbers given by Couhert et al. (2015) derived for Jason-1 and Jason-2 orbits for the second altimetry decade (2002-2012). However, the regional upper bound radial orbit errors obtained from our study are somewhat smaller than the ones reported by Couhert et al. (2015) for the second decade. This might partly reflect recent improvements of the stability of reference frames which result in smaller changes from the ITRF2008 to ITRF2014 reference frame. However, the accuracy of the Earth's time

345 variable gravity model and the tracking observations for the 1990's is inferior to more recent periods. Potentially, the error related to the uncertainties of the tracking station sub-networks is underrated in our study since all analysed orbits rely on basically the same set of tracking observations. For the POD of the GSFC std1504 orbits, Earth's time variable gravity field

has been modelled up to degree and order 5 based on DORIS and SLR data. In the future, POD for the TOPEX period might benefit from further improved Earth's time variable gravity field models making use of DORIS (Cerri et al., 2013) and SLR
350   data (Sośnica et al., 2015).

Acknowledgements

We thank Goddard Space Flight Centre and Groupe de Recherche de Geodesie Spatiale for the provision of GSFC_std1504 and GRGS orbit solutions, ESA CCI for along-track TOPEX Sea Level v1.1 ECV data, and Joana Fenandes for the provision of updated wet troposphere corrections (GPD+). This research was partly supported by the European Space Agency (ESA)
355   within the Climate Change Initiative Sea Level (SLCCI) Phase II project and by the Deutsche Forschungsgemeinschaft (DFG) through grant (CoRSEA) as part of the Special Priority Program (SPP)-1889 "Regional Sea Level Change and Society" (SeaLevel) and within the projects "Consistent dynamic satellite reference frames and terrestrial geodetic datum parameters" and "Interactions of low-orbiting satellites with the surrounding ionosphere and thermosphere (INSIGHT)".

References

360   Ablain, M., Cazenave, A., Valladeau, G. and Guinehut, S.: A new assessment of the error budget of global mean sea level rate estimated by satellite altimetry over 1993–2008, Ocean Sci., 5(2), 193–201, doi:10.5194/os-5-193-2009, 2009.

Ablain, M., Cazenave, A., Larnicol, G., Balmaseda, M., Cipollini, P., Faugère, Y., Fernandes, M. J., Henry, O., Johannessen, J. A., Knudsen, P., Andersen, O., Legeais, J., Meyssignac, B., Picot, N., Roca, M., Rudenko, S., Scharffenberg, M. G., Stammer, D., Timms, G. and Benveniste, J.: Improved sea level record over the satellite altimetry era (1993–2010) from
365   the Climate Change Initiative project, Ocean Sci., 11(1), 67–82, doi:10.5194/os-11-67-2015, 2015.

Ablain, M., Legeais, J. F., Prandi, P., Marcos, M., Fenoglio-Marc, L., Dieng, H. B., Benveniste, J. and Cazenave, A.: Satellite Altimetry-Based Sea Level at Global and Regional Scales, Surv. Geophys., 1–25, doi:10.1007/s10712-016-9389-8, 2016.

Altamimi, Z., Collilieux, X. and Métivier, L.: ITRF2008: an improved solution of the international terrestrial reference frame, J. Geod., 85(8), 457–473, doi:10.1007/s00190-011-0444-4, 2011.

370   Altamimi, Z., Rebischung, P., Métivier, L. and Collilieux, X.: ITRF2014: A new release of the International Terrestrial Reference Frame modeling nonlinear station motions, J. Geophys. Res. Solid Earth, 121(8), 2016JB013098, doi:10.1002/2016JB013098, 2016.

Beckley, B., Ray, R., Holmes, S., Zelensky, N., Lemoine, F., Yang, X., Brown, S., Desai, S., Mitchum, G. and Hausman, J.: Integrated Multi-Mission Ocean Altimeter Data for Climate Research TOPEX/Poseidon, Jason-1 and OSTM/Jason-2
375   User's   Handbook   Version   3.0,   pp.   61,   California   Institute   of   Technology, ftp://podaac.jpl.nasa.gov/allData/merged_alt/L2/TP_J1_OSTM/docs/v121415.version3.0_multi_alt_handbook.pdf (Accessed May 2017), 2015.

Boehm, J. and Schuh, H.: Vienna mapping functions in VLBI analyses, Geophys. Res. Lett., 31(1), L01603, doi:10.1029/2003GL018984, 2004.

380   Carrère, L., Lyard, F., Cancet, M., Roblou, L. and Guillot, A.: FES 2012: a new tidal model taking advantage of nearly 20
        years of altimetry measurements, OSTST meeting, September 22-29, Venice-Lido, Italy, [online] Available from:
        http://www.aviso.altimetry.fr/fileadmin/documents/OSTST/2012/oral/01_thursday_27/03_tides/04_TID_Carrere2.pdf
        (Accessed May 2017), 2012.

        Cazenave, A., Dieng, H.-B., Meyssignac, B., von Schuckmann, K., Decharme, B. and Berthier, E.: The rate of sea-level rise,
385   Nature Clim. Change, 4(5), 358–361, doi:10.1038/nclimate2159, 2014.

        Cerri, L. and Ferrage, P.: DORIS satellites models implemented in POE processing, CNES, Paris, France, Tech. Rep. SALP-
        NTBORD-OP-16137-CN,   Rev.   10,   [online]   Available   from: ftp://ftp.ids-
        doris.org/pub/ids/satellites/DORISSatelliteModels.pdf (Accessed May 2017), 2016.

        Cerri, L., Lemoine, J. M., Mercier, F., Zelensky, N. P. and Lemoine, F. G.: DORIS-based point mascons for the long term
390   stability of precise orbit solutions, Adv. Space Res., 52(3), 466–476, doi:10.1016/j.asr.2013.03.023, 2013.

        Church, J. A. and White, N. J.: Sea-Level Rise from the Late 19th to the Early 21st Century, Surv. Geophys., 32(4–5), 585–
        602, doi:10.1007/s10712-011-9119-1, 2011.

        Couhert, A., Cerri, L., Legeais, J.-F., Ablain, M., Zelensky, N. P., Haines, B. J., Lemoine, F. G., Bertiger, W. I., Desai, S. D.
        and Otten, M.: Towards the 1 mm/y stability of the radial orbit error at regional scales, Adv. Space Res., 55(1), 2–23,
395   doi:10.1016/j.asr.2014.06.041, 2015.

        Dobslaw, H., Flechtner, F., Bergmann-Wolf, I., Dahle, C., Dill, R., Esselborn, S., Sasgen, I. and Thomas, M.: Simulating
        high-frequency atmosphere-ocean mass variability for dealiasing of satellite gravity observations: AOD1B RL05, J.
        Geophys. Res. Oceans, 118(7), 3704–3711, doi:10.1002/jgrc.20271, 2013.

        Douglas, B. C.: Global Sea Rise: A Redetermination, Surv. Geophys., 18(2–3), 279–292, doi:10.1023/A:1006544227856,
400   1997.

        Esselborn, S., Schöne, T. and Rudenko, S.: Impact of Time Variable Gravity on Annual Sea Level Variability from Altimetry,
        in IAG 150 Years, pp. 55–62, Springer, Cham., doi:10.1007/1345_2015_103, 2015.

        Fasullo, J. T., Nerem, R. S. and Hamlington, B.: Is the detection of accelerated sea level rise imminent?, Scientific Reports,
        6, 31245, doi:10.1038/srep31245, 2016.

405   Fernandes, M. J. and Lázaro, C.: GPD+ Wet Tropospheric Corrections for CryoSat-2 and GFO Altimetry Missions, Remote
        Sensing, 8(10), 851, doi:10.3390/rs8100851, 2016.

        Förste, C., Bruinsma, S., Abrikosov, O., Rudenko, S., Lemoine, J.-M., Marty, J.-C., Neumayer, K. H. and Biancale, R.:
        EIGEN-6S4 A time-variable satellite-only gravity field model to d/o 300 based on LAGEOS, GRACE and GOCE data
        from   the   collaboration   of   GFZ   Potsdam   and   GRGS   Toulouse,   [online]   Available   from:
410   https://doi.org/10.5880/icgem.2016.008 (Accessed May 2017), 2016.

        Fu, L.-L. and Haines, B. J.: The challenges in long-term altimetry calibration for addressing the problem of global sea level
        change, Adv. Space Res., 51(8), 1284–1300, doi:10.1016/j.asr.2012.06.005, 2013.

        Goiginger, H., Hoeck, E., Rieser, D., Mayer-Guerr, T., Maier, A., Krauss, S., Pail, R., Fecher, T., Gruber, T. and Brockmann,
        J.: The combined satellite-only global gravity field model GOCO02S, Geophysical Research Abstracts, 13, EGU2011-
415   10571, [online] Available from: http://www.goco.eu/data/egu2011-10571-goco02s.pdf (Accessed May 2017), 2011.

Hedin, A. E.: MSIS-86 Thermospheric Model, J. Geophys. Res.: Space Physics, 92(A5), 4649–4662, doi:10.1029/JA092iA05p04649, 1987.

Hay, C. C., Morrow, E., Kopp, R. E. and Mitrovica, J. X.: Probabilistic reanalysis of twentieth-century sea-level rise, Nature, 517(7535), 481–484, doi:10.1038/nature14093, 2015.

420 IERS Conventions (2003), McCarthy, D.D. and Petit, G. (Eds.): Bundesamt für Kartographie und Geodäsie, Frankfurt am Main. [online] Available from: http://www.iers.org/TN32 (Accessed May 2017), 2004.

IERS Conventions (2010), Petit, G. and Luzum, B. (Eds.): Bundesamt für Kartographie und Geodäsie, Frankfurt am Main. [online] Available from: https://www.iers.org/TN36 (Accessed May 2017), 2010.

Jevrejeva, S., Moore, J. C., Grinsted, A. and Woodworth, P. L.: Recent global sea level acceleration started over 200 years
425 ago?, Geophys. Res. Lett., 35(8), L08715, doi:10.1029/2008GL033611, 2008.

Jevrejeva, S., Moore, J. C., Grinsted, A., Matthews, A. P. and Spada, G.: Trends and acceleration in global and regional sea levels since 1807, Global and Planetary Change, 113, 11–22, doi:10.1016/j.gloplacha.2013.12.004, 2014.

Knocke, P. and Ries, J.: Earth Radiation Pressure Effects on Satellites, Technical Memorandum, Center for Space Research, the University of Texas at Austin, Austin, Texas, 1987.

430 Knocke, P., Ries, J. and Tapley, B.: Earth radiation pressure effects on satellites, in AIAA Paper 88-4292, pp. 577–587, Austin, TX, United States, 1988.

Lemoine, F. G., Zelensky, N. P., Chinn, D. S., Pavlis, D. E., Rowlands, D. D., Beckley, B. D., Luthcke, S. B., Willis, P., Ziebart, M., Sibthorpe, A., Boy, J. P. and Luceri, V.: Towards development of a consistent orbit series for TOPEX, Jason-1, and Jason-2, Adv. Space Res., 46(12), 1513–1540, doi:10.1016/j.asr.2010.05.007, 2010.

435 Lemoine, F. G., Chinn, D. S., Zelensky, N. P., Beall, J. W. and Le Bail, K.: The development of the GSFC DORIS contribution to ITRF2014, Adv. Space Res., 58(12), 2520–2542, doi:10.1016/j.asr.2015.12.043, 2016.

Llovel, W., Becker, M., Cazenave, A., Jevrejeva, S., Alkama, R., Decharme, B., Douville, H., Ablain, M. and Beckley, B.: Terrestrial waters and sea level variations on interannual time scale, Glob. Planet. Change, 75(1–2), 76–82, doi: 10.1016/j.gloplacha.2010.10.008, 2011.

440 Lyard, F., Lefevre, F., Letellier, T. and Francis, O.: Modelling the global ocean tides: modern insights from FES2004, Ocean Dyn., 56(5–6), 394–415, doi:10.1007/s10236-006-0086-x, 2006.

Masters, D., Nerem, R. S., Choe, C., Leuliette, E., Beckley, B., White, N. and Ablain, M.: Comparison of Global Mean Sea Level Time Series from TOPEX/Poseidon, Jason-1, and Jason-2, Marine Geodesy, 35(sup1), 20–41, doi:10.1080/01490419.2012.717862, 2012.

445 Melachroinos, S. A., Lemoine, F. G., Zelensky, N. P., Rowlands, D. D., Luthcke, S. B. and Bordyugov, O.: The effect of geocenter motion on Jason-2 orbits and the mean sea level, Adv. Space Res., 51(8), 1323–1334, doi:10.1016/j.asr.2012.06.004, 2013.

Mendes, V. B. and Pavlis, E. C.: High-accuracy zenith delay prediction at optical wavelengths, Geophys. Res. Lett., 31(14), L14602, doi:10.1029/2004GL020308, 2004.

450 Pavlis, E. C., SLRF2008: The ILRS reference frame for SLR POD contributed to ITRF2008, presented at the Ocean Surf. Topogr. Sci. Team Meeting, Seattle, WA, USA, Jun. 2009. [online] Available from: http://www.aviso.oceanobs.com/fileadmin/documents/OSTST/2009/poster/Pavlis_2.pdf (Accessed May 2017), 2009.

Ray, R. D.: Precise comparisons of bottom-pressure and altimetric ocean tides, J. Geophys. Res. Oceans, 118(9), 4570–4584, doi:10.1002/jgrc.20336, 2013.

455 Ries, J.: Annual geocenter motion from space geodesy and models, abstract G12A-08, AGU Fall Meeting, San Francisco, 9-13 December 2013, [online] Available from: http://ids-doris.org/images/documents/report/publications/AGU2013-AnnualGeocenterMotion-Ries.pdf (Accessed May 2017), 2013.

Rudenko, S., Otten, M., Visser, P., Scharroo, R., Schöne, T. and Esselborn, S.: New improved orbit solutions for the ERS-1 and ERS-2 satellites, Adv. Space Res., 49(8), 1229–1244, doi:10.1016/j.asr.2012.01.021, 2012.

460 Rudenko, S., Dettmering, D., Esselborn, S., Schöne, T., Förste, C., Lemoine, J.-M., Ablain, M., Alexandre, D. and Neumayer, K.-H.: Influence of time variable geopotential models on precise orbits of altimetry satellites, global and regional mean sea level trends, Adv. Space Res., 54(1), 92–118, doi:10.1016/j.asr.2014.03.010, 2014.

Rudenko, S., Dettmering, D., Esselborn, S., Fagiolini, E. and Schöne, T.: Impact of Atmospheric and Oceanic De-aliasing Level-1B (AOD1B) products on precise orbits of altimetry satellites and altimetry results, Geophys. J. Int., 204(3), 1695–
465 1702, doi:10.1093/gji/ggv545, 2016.

Rudenko, S., Neumayer, K.-H, Dettmering, D., Esselborn, S., Schöne, T. and Raimondo, J.-C.: Improvements in precise orbits of altimetry satellites and their impact on mean sea level monitoring, IEEE Trans. Geosci. Remote Sens., 55(6), 3382-3395, doi:10.1109/TGRS.2017.2670061, 2017.

Savcenko, R. and Bosch, W.: EOT11a-empirical ocean tide model from multi-mission satellite altimetry, DGFI Report 89,
470 [online] Available from: http://epic.awi.de/36001/1/DGFI_Report_89.pdf (Accessed May 2017), 2012.

Schöne, T., Esselborn, S., Rudenko, S. and Raimondo, J.-C.: Radar Altimetry Derived Sea Level Anomalies – The Benefit of New Orbits and Harmonization, in System Earth via Geodetic-Geophysical Space Techniques, edited by F. M. Flechtner, T. Gruber, A. Güntner, M. Mandea, M. Rothacher, T. Schöne, and J. Wickert, pp. 317–324, Springer Berlin Heidelberg, Berlin, Heidelberg. [online] Available from: http://edoc.gfz-potsdam.de/gfz/16014 (Accessed May 2017), 2010.

475 Sośnica, K., Jäggi, A., Meyer, U., Thaller, D., Beutler, G., Arnold, D. and Dach, R.: Time variable Earth's gravity field from SLR satellites, J. Geod., 1–16, doi:10.1007/s00190-015-0825-1, 2015.

Soudarin, L., Capdeville, H. and Lemoine, J.-M.: Activity of the CNES/CLS Analysis Center for the IDS contribution to ITRF2014, Adv. Space Res., 58(12), 2543–2560, doi:10.1016/j.asr.2016.08.006, 2016.

Watson, C. S., White, N. J., Church, J. A., King, M. A., Burgette, R. J. and Legresy, B.: Unabated global mean sea-level rise
480 over the satellite altimeter era, Nature Clim. Change, 5(6), 565–568, doi:10.1038/nclimate2635, 2015.

Willis, P., Zelensky, N. P., Ries, J., Soudarin, L., Cerri, L., Moreaux, G., Lemoine, F. G., Otten, M., Argus, D. F. and Heflin, M. B.: DPOD2008: A DORIS-Oriented Terrestrial Reference Frame for Precise Orbit Determination, in IAG 150 Years, pp. 175–181, Springer, Cham., doi: 10.1007/1345_2015_125, 2015.

485

490

Table 1. The main models used for calculation of GFZ VER11, GSFC std1504 and GRGS orbits

Parameter	GFZ REF (VER11) orbit	GSFC std1504 orbit	GRGS orbit
Terrestrial reference frame	ITRF2008 (Altamimi et al., 2011), SLRF2008 (Pavlis 2009), DPOD2008 (Willis et al., 2016)	ITRF2008, SLRF2008, DPOD2008	ITRF2008, SLRF2008, DPOD2008
Polar motion and UT1	IERS EOP 08 C04 (IAU2000A) series with IERS diurnal and semi-diurnal variations	IERS Bulletin A daily (consistent with ITRF2008), diurnal and semi-diurnal variations	IERS EOP 08 C04
Precession and nutation model	IERS Conventions (2010)	IAU2000	IERS 2010 using non-rotating origin
Station displacements due to annual geocenter variations	None	Ries (2013)	None
Non-tidal atmospheric loading effect on stations	Based on ECMWF ERA-Interim data	None	None
Ocean loading effect on stations	FES2004 (Lyard at al., 2006)	GOT4.10 (Ray, 2013)	FES2012 (Carrère et al., 2012)
Static Earth's gravity field model	EIGEN-6S4 (Förste et al., 2016) degree/order 81-90	GOCO2S (> L=5) (Goiginger et al., 2011)	EIGEN-6S2 (Rudenko et al., 2014)
Time-variable Earth's gravity field model	EIGEN-6S4 up to d/o 80	Updated harmonic piece-wise fit weekly solutions (Lemoine et al., 2016) up to d/o 5	EIGEN-6S2 up to d/o 50
Solid Earth tide	IERS Conventions (2010)	IERS Conventions (2003)	IERS Conventions (2010)
Ocean tide model	EOT11a (Savchenko and Bosch, 2012) up to d/o 80	GOT4.10 up to d/o 50	FES2012 up to d/o 50
Non-tidal atmospheric and oceanic gravity	GFZ AOD1B RL05 (Dobslaw et al, 2013) ECMWF 6-hourly fields up to d/o 100	ECMWF 6-hourly fields up to d/o 50	3-hourly ERA-interim and TUGO R12 up to d/o 50
Atmospheric density model	MSIS-86 (Hedin, 1987)	MSIS-86	DTM 94, with best available solar activity data
Earth radiation and albedo	Knocke and Ries (1987)	Knocke et al. (1988)	Albedo and IR pressure values interpolated from ECMWF 6hr grids

Radiation pressure model	Tuned 8-panel (Cerri and Ferrage, 2014)	Tuned 8-panel	Thermo-optical coefficient from pre-launch box and wing model, with smoothed Earth shadow model
Tracking data	SLR, DORIS	SLR, DORIS	SLR, DORIS
SLR tropospheric correction model	IERS Conventions (2010)	Mendes and Pavlis (2004)	IERS Conventions (2010)
DORIS tropospheric correction model	Vienna Mapping Functions 1 (Boehm and Schuh, 2004)	Vienna Mapping Functions 1	GPT2/Vienna Mapping Functions 1
DORIS modelling	DORIS beacon frequency bias modelling	DORIS beacon phase center	DORIS beacon phase center
SLR antenna reference	LRA model (note 1 below)	LRA model (note 1 below)	X: 1.2429, Y: -0.0012, Z: 0.8783 in [m]
DORIS antenna reference	pre-launch	pre-launch	pre-launch
SLR / DORIS observation weight	3 cm / 0.05 cm/s	10 cm / 0.2 cm/s	1 cm / 0.03 cm/s

Note 1: https://ilrs.cddis.eosdis.nasa.gov/missions/satellite_missions/past_missions/topx_com.html

Table 2. Average values of SLR and DORIS RMS fits, radial, cross-track and along-track two-day arc overlaps and the number of the arcs used to compute these values for the reference and four test orbits.

Orbit name	SLR RMS [cm]	DORIS RMS [cm/s]	Radial arc overlap [cm]	Cross-track arc overlap [cm]	Along-track arc overlap [cm]	Number of arcs used for SLR RMS	Number of arcs used for DORIS RMS	Number of arc overlaps used	Comment on the orbit
REF	1.96	0.04778	0.90	6.52	3.65	494	459	433	Reference
SLR	1.59		1.72	7.23	9.54	494		425	SLR only
DORIS		0.04795	0.88	6.84	2.96		459	392	DORIS only
ITRF14	1.97	0.04776	0.84	6.45	2.83	494	459	433	ITRF2014
Geoid	1.96	0.04775	0.83	6.43	2.80	494	459	433	EIGEN-6S2

Table 3: Median of time series of global mean height differences and RMS values at crossover points for maximum time lapses of 5
days for all orbit solutions during the period April 1993 ─ November 2004. The highest and lowest values of each quantity are
marked bold.

	REF	GSFC	GRGS	SLR	DORIS	ITRF14	Geoid
Mean [mm]	-3.1	**-1.6**	-2.9	-2.6	**-4.7**	-3.1	-2.1
RMS [mm]	49.8	**49.5**	**51.3**	51.1	50.7	49.8	49.7

Table 4: Global mean orbit related errors for the total signal, interannual trend variability, and decadal trend. Values were derived
from the mean radial orbit differences over the oceans: *REF minus SLR*, *REF minus DORIS*, *REF minus ITRF14*, *REF minus
Geoid*, *REF minus GSFC*, *REF minus GRGS* for the period April 1993 ─ June 2004. The corresponding values for the total sea level
are tabulated under SLA.

	REF-SLR	REF-DORIS	REF-ITRF2014	REF-Geoid	REF-GSFC	REF-GRGS	SLA
RMS [mm]	4.2	5.1	1.1	2.0	5.4	7.0	52.5
5-years trend [mm/year]	0.04	0.10	0.02	0.02	0.05	0.10	0.55
Decadal trend [mm/year]	0.01	0.05	0.00	0.00	0.04	0.02	2.89

Table 5: Regional orbit related errors for the total and seasonal signal, for interannual trend variability and decadal trend. Values
were derived from the radial orbit differences: *REF minus SLR*, *REF minus DORIS*, *REF minus ITRF14*, *REF minus Geoid*, *REF
minus GSFC*, *REF minus GRGS* for the periods April 1993 ─ June 2004.

	REF-SLR	REF-DORIS	REF-ITRF2014	REF-GEOID	REF-GSFC	REF-GRGS
RMS [mm]	7.2	9.3	2.4	3.5	7.4	10.7
Annual amplitude [mm]	1.4	2.1	0.4	3.2	5.4	5.6
5-years trend [mm/year]	0.5	0.6	0.2	0.4	1.2	0.9
Decadal trend [mm/year]	0.2	0.4	0.2	0.4	1.0	0.7

Table 6: Global mean differences of interannual trend variability and decadal trend related to the orbit solution. Values were
derived from the mean radial orbit differences over the oceans: *REF minus SLR*, *REF minus DORIS* and *Geoid minus GRGS* for
the period April 1993 ─ June 2004 from all tracks and (in brackets) for ascending, descending tracks separately.

	REF-SLR	REF-DORIS	Geoid-GRGS
Interannual trend [mm/year]	0.04 (0.30, 0.25)	0.10 (0.53, 0.37)	0.05 (0.36, 0.29)
Decadal trend [mm/year]	0.01 (-0.07, 0.07)	-0.05 (0.19, -0.27)	-0.01 (0.28, -0.34)

515
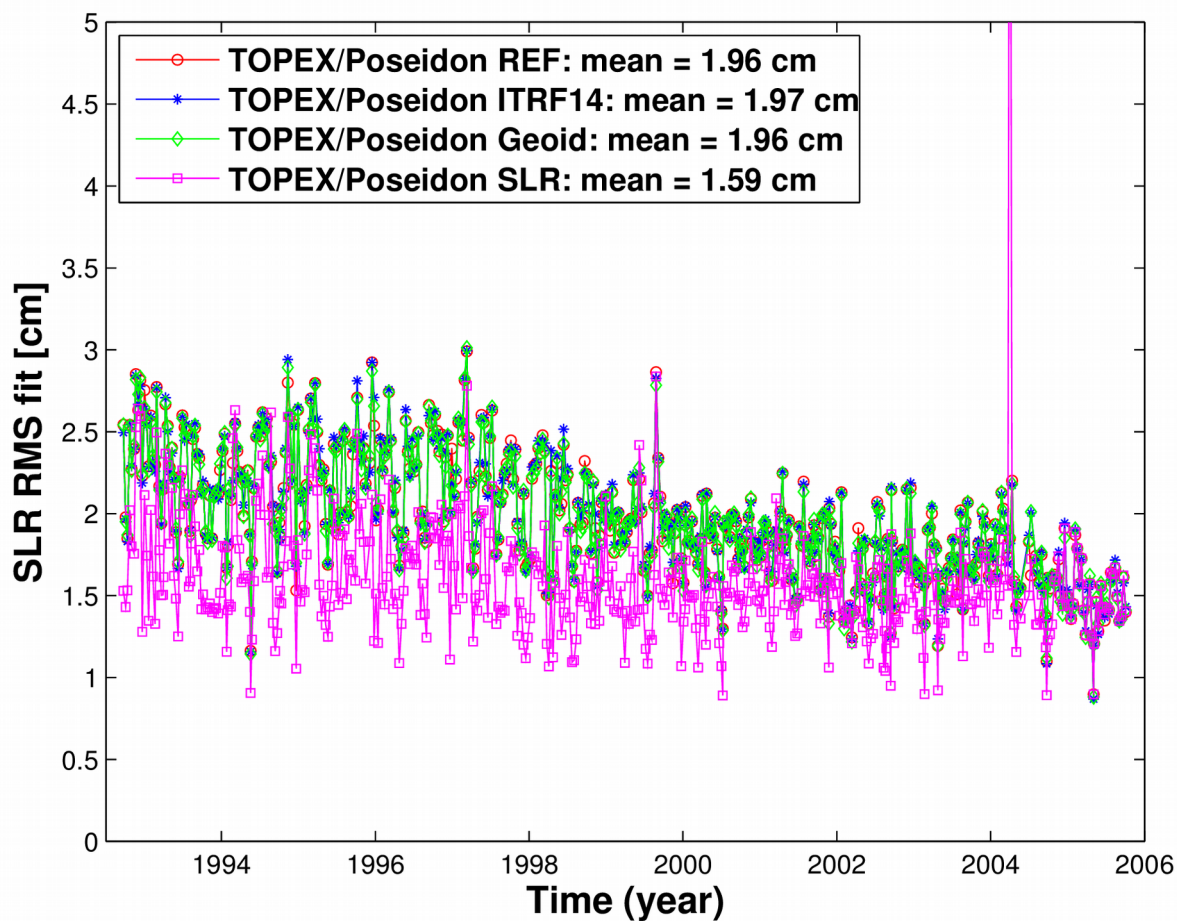
Figure 1: SLR RMS fits of TOPEX/Poseidon REF, SLR, ITRF14, and Geoid orbits.

520

525
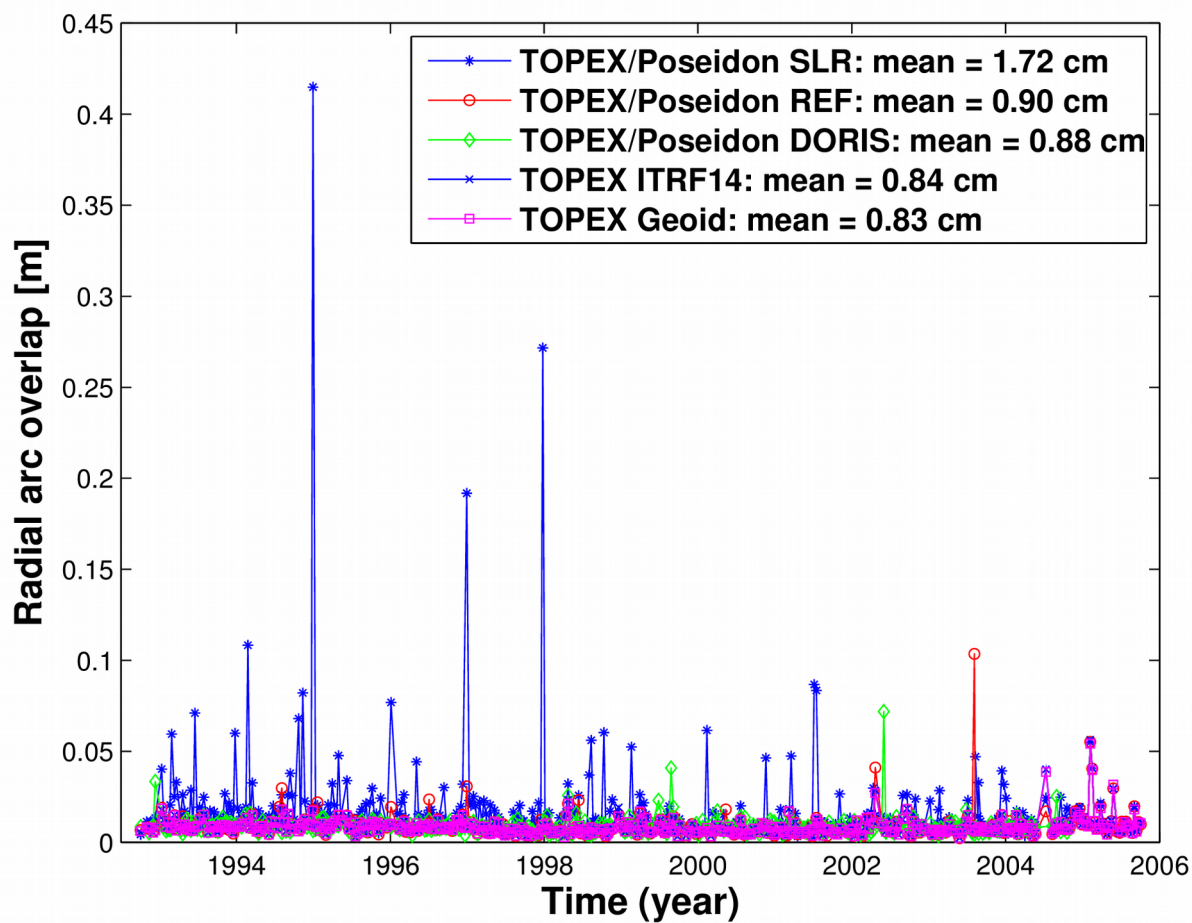
Figure 2. Radial arc overlaps of TOPEX/Poseidon REF, SLR, DORIS, ITRF14, and Geoid orbits.

530

535
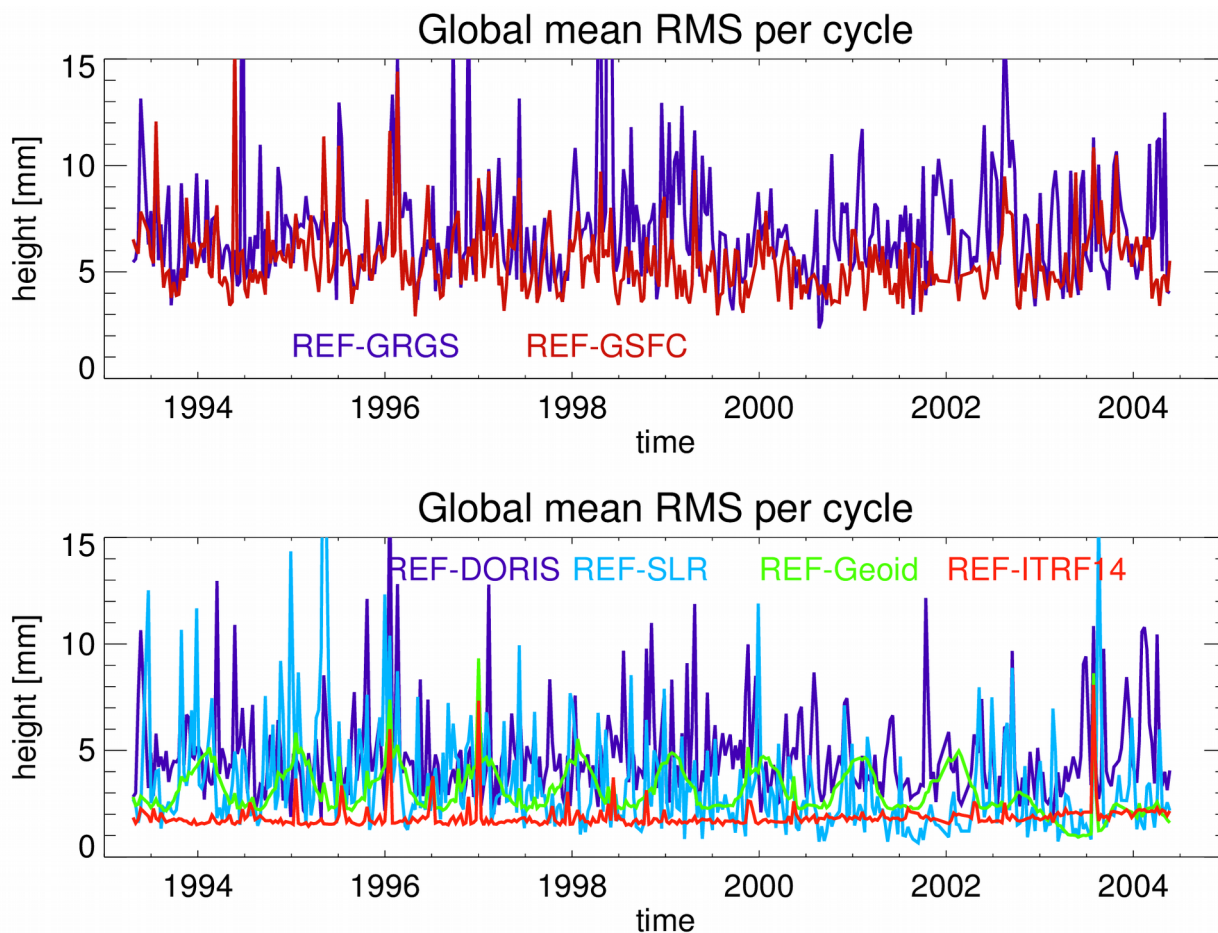
Figure 3: Time series of the global mean RMS per cycle over the oceans of gridded radial orbit differences for *REF minus GSFC*
(dark blue), and *REF minus GRGS* (red) on the top; for *REF minus DORIS* (dark blue), *REF minus SLR* (light blue), *REF minus*
Geoid (green), and *REF minus ITRF2014* (red) on the bottom.

540

545
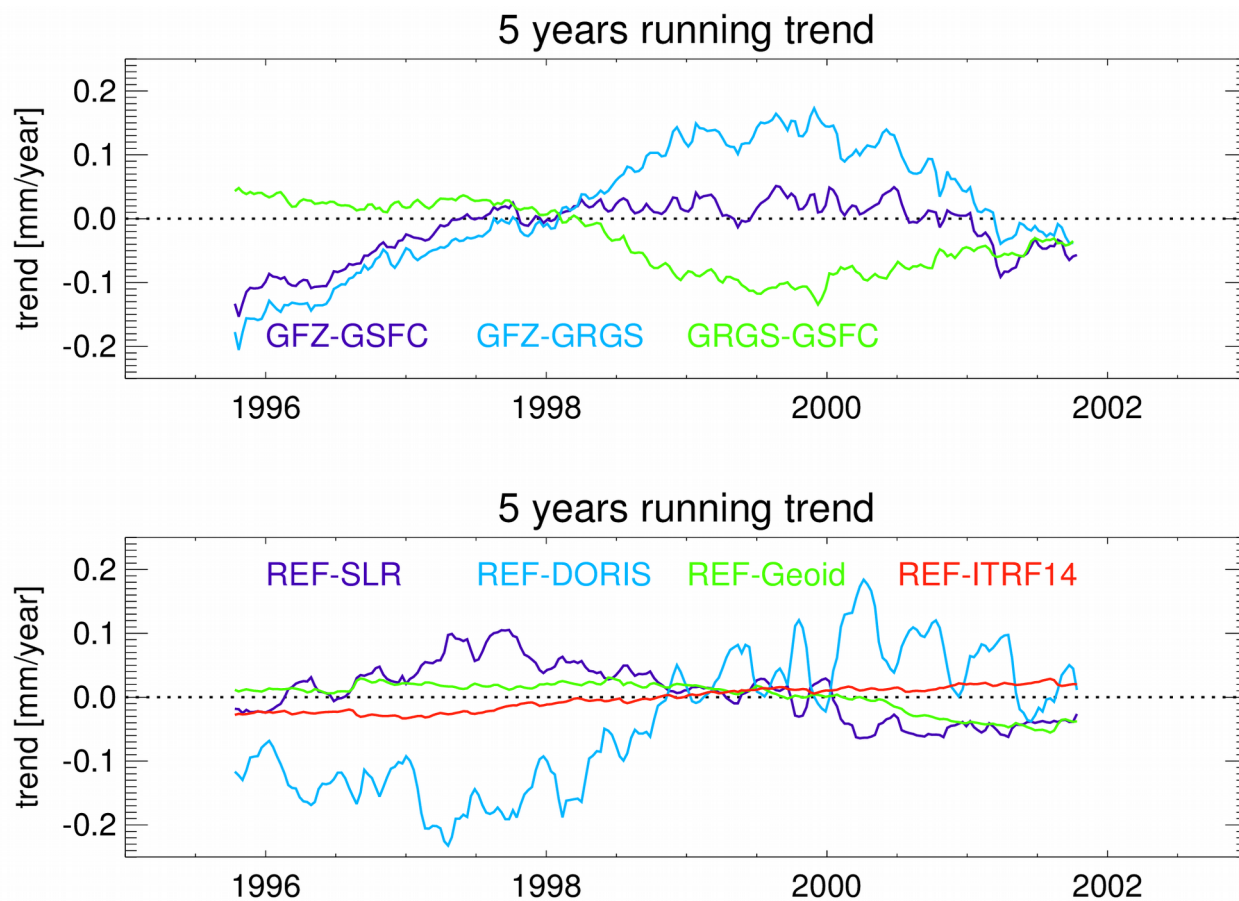
Figure 4: 5-years running trends for the global mean radial orbit differences over the oceans for *REF minus GSFC* (dark blue), *REF minus GRGS* (light blue), and *GRGS minus GSFC* (green) on the top; for *REF minus SLR* (dark blue), *REF minus DORIS* (light blue), *REF minus Geoid* (green), and R*EF minus ITRF14* (red) on the bottom.
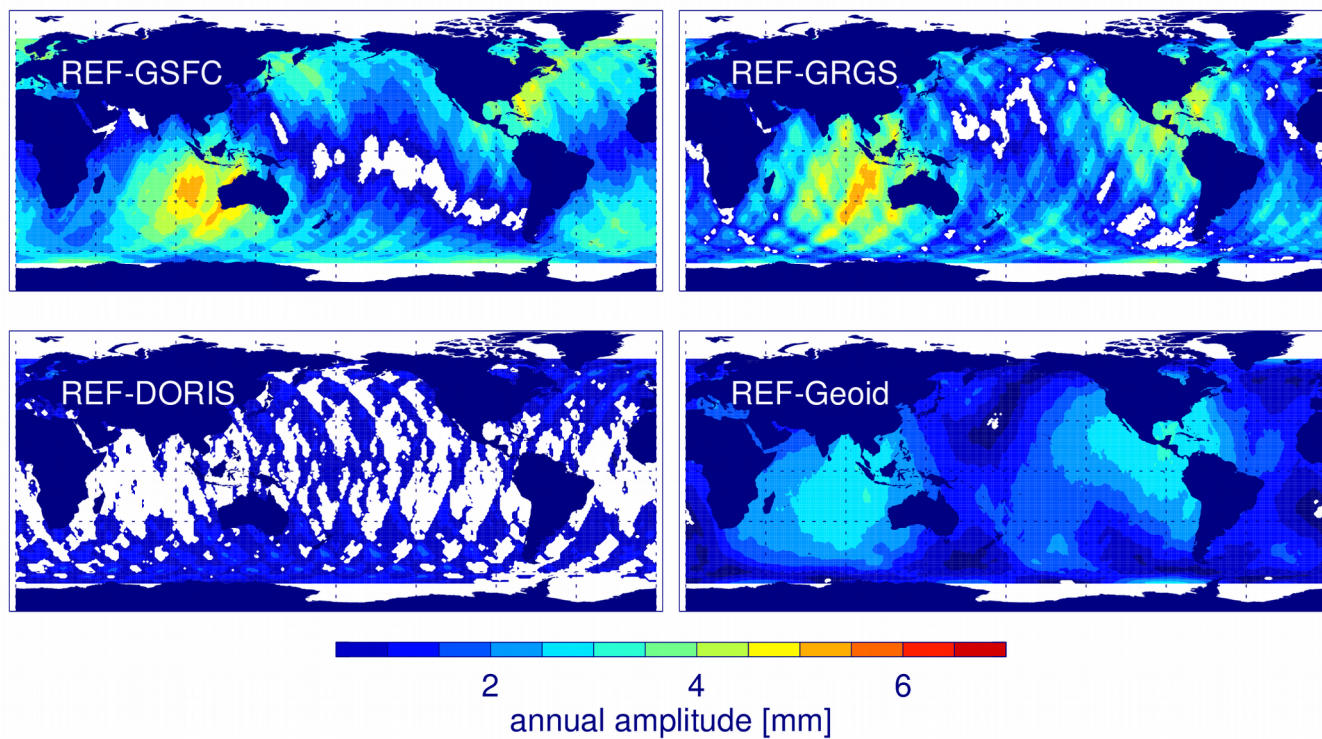
Figure 5: Annual amplitude of the radial orbit differences for *REF minus GSFC*, *REF minus GRGS*, *REF minus DORIS*, and *REF minus Geoid*. The regions with formal errors larger than the fitted value are masked out (white). The maximum amplitude difference is given in Table 5.

565

570

575
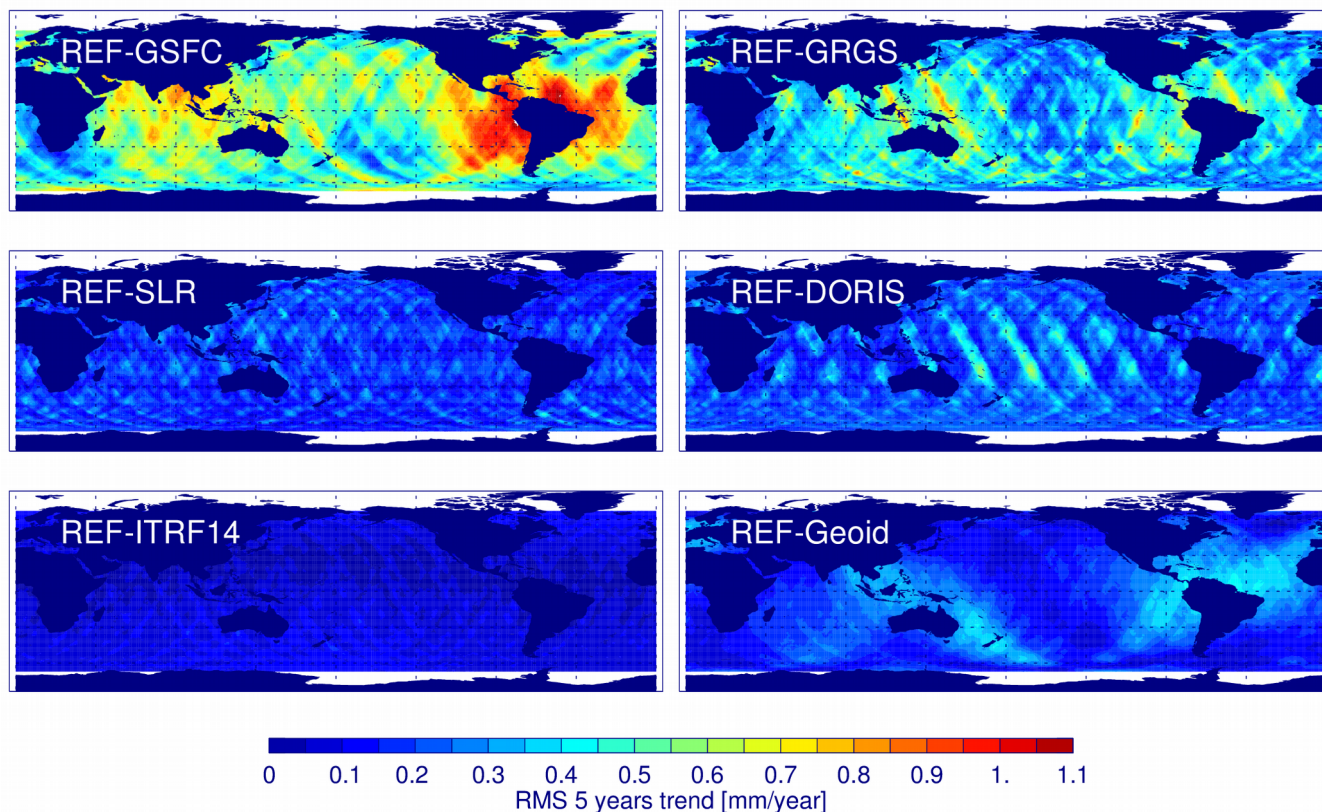
Figure 6: RMS of 5-years running trend differences of the radial orbit components for *REF minus GSFC*, *REF minus GRGS*, *REF minus SLR*, *REF minus DORIS*, *REF minus ITRF14*, and *REF minus Geoid* for the period April 1993 ─ June 2004. The global mean RMS of the differences over the ocean is given in Table 4.
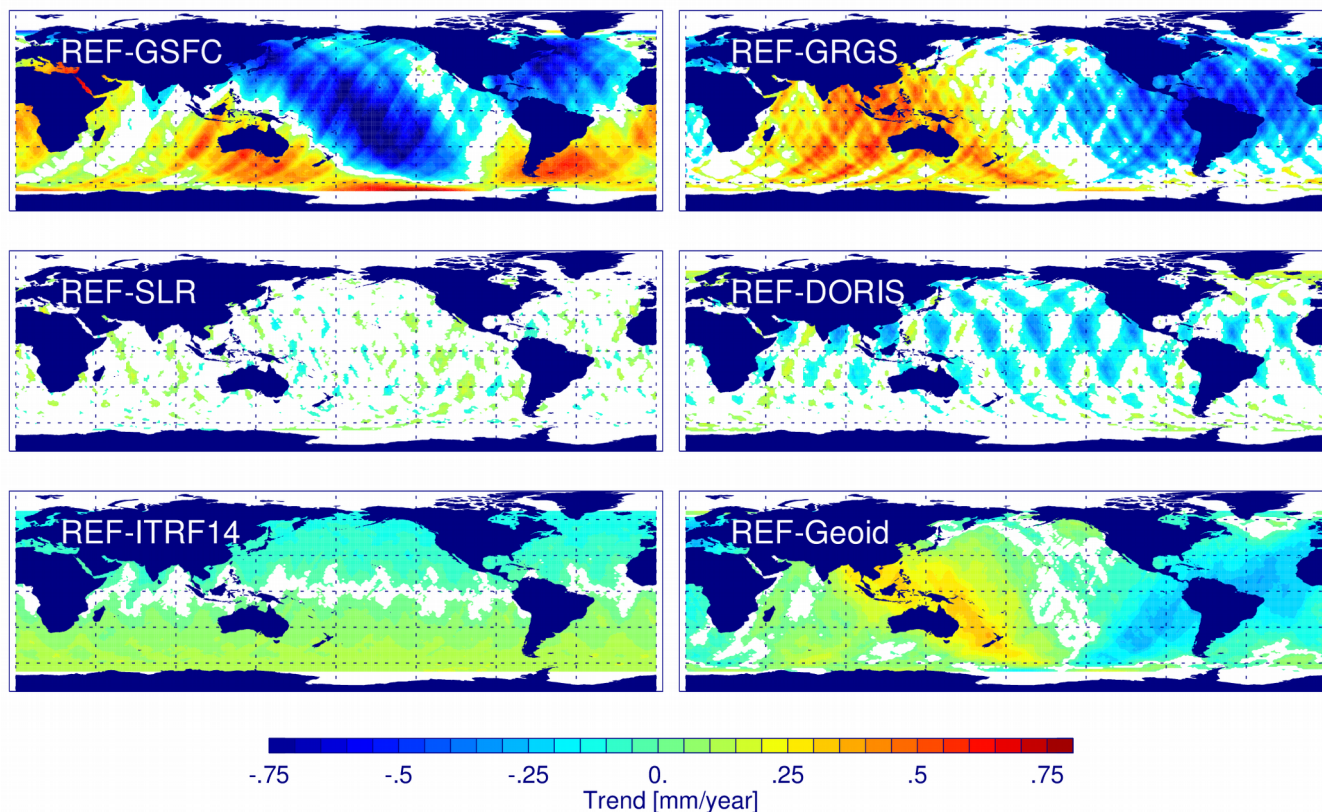
Figure 7: Trend differences of radial orbit components for *REF minus GSFC*, *REF minus GRGS*, *REF minus SLR*, *REF minus DORIS*, *REF minus ITRF14*, and *REF minus Geoid* for the period April 1993─June 2004. Regions with formal errors larger than the fitted value are masked out (white). The global mean trend difference over the ocean is given in Table 4.
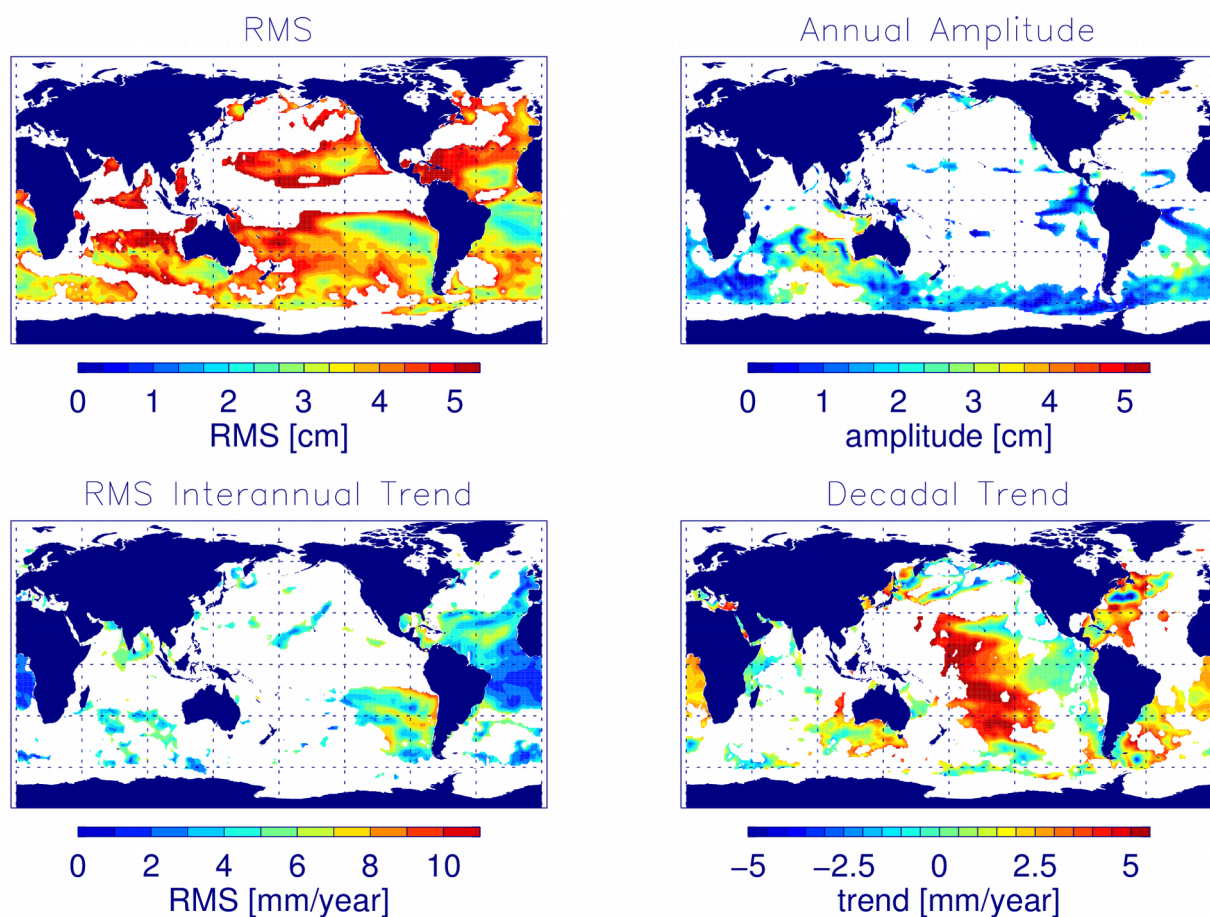
Figure 8: RMS of sea level, annual amplitude, RMS of interannual (5 years) running trend, and decadal trends from TOPEX altimeter data for the period February 1993─ October 2005. Colour coded are sea level values for which the local orbit errors
610 **(estimated from *GFZ minus GRGS)* reach more than 10 % of the local sea level values. All other regions are masked out (white).**

615
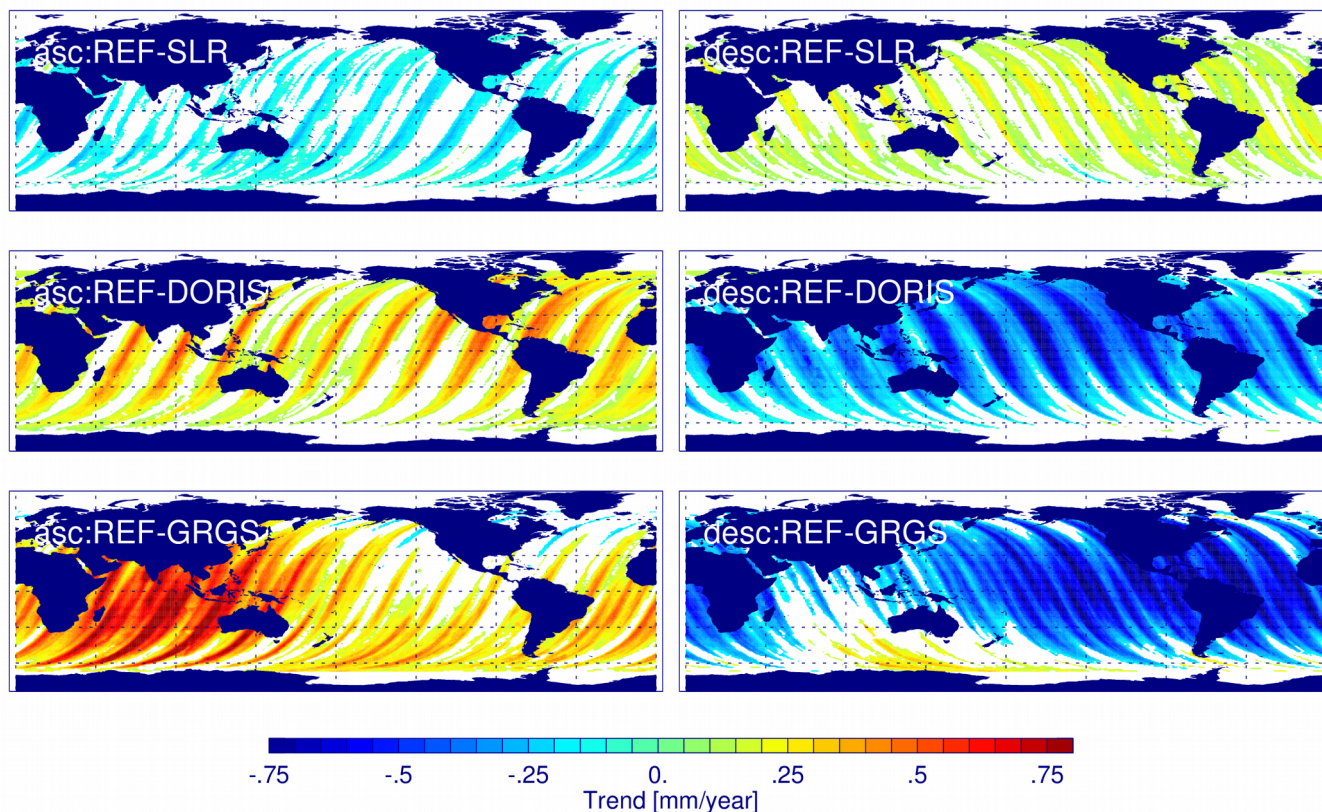
Figure 9: Trend differences of radial orbit components for ascending (left) and descending (right) tracks for *REF minus SLR*, *REF minus DORIS*, and *Geoid minus GRGS* for the period April 1993 − June 2004. Regions with formal errors larger than the fitted value are masked out (white). The global mean trend difference over the ocean is given in Table 6.